Journal Name

ARTICLE

Microsecond resolution of cavitation bubble dynamics using a high-speed electrochemical impedance approach

Received 00th January 20xx,
Accepted 00th January 20xx

DOI: 10.1039/x0xx00000x

www.rsc.org/

P. R. Birkin[a†], T. M. Foley[a], J. L. Barber[a] and H. L. Martin[a]

A new method to detect the uncompensated resistance, the capacitance and the Faradaic current at an electrode exposed to ultrasonic cavitation is presented. The method enables these parameters to be resolved with a 2 microsecond resolution and relies on the detection of the impedance of an electrode recorded as a function of time with a suitable AC excitation signal (here 500 kHz). Data obtained from an aluminium electrode, held under potentiostatic control, is used to illustrate the technique with particular relevance to the effects of cavitation bubbles generated by ultrasound. Analysis of the data recorded shows that the cavitation bubbles form close to the surface of the electrode and collapse, causing damage to the passive film formed at the aluminium surface. The capacitance, uncompensated resistance and Faradaic signals are used to explore the dynamic processes and show expansion and collapse of bubbles prior to erosion/corrosion. The close proximity of the bubbles to the surface is deduced from the reductions in capacitance and increases in resistance prior to bubble collapse, which is then shown to trigger the onset of a Faradaic signal, thus confirming the erosion/corrosion mechanism previously assumed.

Introduction

Gas bubbles in liquids can be produced and activated in a variety of ways; these include natural phenomena where flow fields entrap or induce bubble activity; they can be generated through the application of a suitable forcing regime (for example an ultrasonic field[1]) or they can be produced by chemical and electrochemical reactions[2–4]. Cavitation effects are also generated in the natural world by a variety of organisms; including the mantis shrimp which are thought to use this phenomenon[5,6]. From a technological perspective, the generation of cavitation can be extremely useful for cleaning surfaces[7–10] and for the generation of unusual chemical[11,12] and physical effects[13,14] in liquids with an ambient bulk temperature. These effects can be extreme with high localised temperatures and pressures (often quoted[11] in the many 1000s of Kelvin and 100s of atmospheres[12,15]) resulting from the collapse phase of bubbles generated during these experiments. These unusual conditions have been harnessed and used in the broad field of sonochemistry for the destruction of toxic materials[16,17] or the generation of particles, for example[18,19]. However, although this inertial cavitation process can be useful, it is also an extremely difficult phenomenon to fully characterise[20,21]. This is because the dynamics of the processes involved are often in the µs time domain, the effects are extremely local[11] and the media is often opaque due to the dynamic nature of the bubbles produced and the myriad of events generated at one time[22]. Furthermore, it is desirable to have a physically non-invasive characterisation technique. Hence, to the experimentalist, these systems pose an interesting challenge while pertaining to be of significant use if the processes can be optimised for a particular application. Thus many different approaches involving high-speed imaging[13], acoustic measurements[23], chemical measurements[16], photonic characterisation[24] and the study of surface damage are among the studies that can be found in the literature[1]. Amongst the measurement techniques available, electrochemical characterisation of cavitation is noteworthy[25]. The data obtained from an electrochemical investigation can be broadly assigned to the characterisation of three main areas, specifically surface damage[26–29], mass transfer of material[25,30,31] or chemical change[16]. Unfortunately,

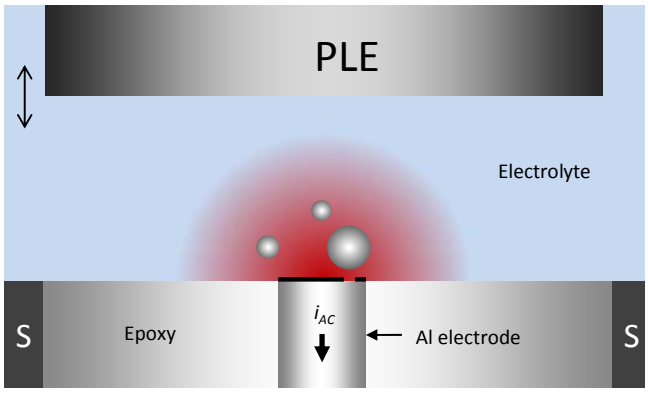

Figure 1. Schematic representation of the generation of bubbles close to the electrode surface by an operating ultrasonic source (PLE, ↕ shows vibrating motion). 'S' represents the stainless steel reference/support. These perturb the environment above the electrode and are detected as a change in the measured uncompensated resistance and the apparent capacitance of the electrode. Events that damage the passive layer (here in black) cause an additional Faradaic current which can be extracted from the current (i_{AC}). Not to scale.

[a] Chemistry, University of Southampton, Southampton, SO17 1BJ, UK.
† Author for correspondence.
Electronic Supplementary Information (ESI) available: [details of any supplementary information available should be included here]. See DOI: 10.1039/x0xx00000x

without complementary data[32,33] or more elaborate electrode geometries[33], electrochemistry on its own can only provide some of the experimental evidence needed to fully understand these complex environments. For example, mass transfer can be stimulated in these cavitation systems by bubble motion[34], bubble oscillation[33,35] and bubble collapse[13] while surface damage has been attributed to bubble collapse and shock generation[13]. In all cases rich current time histories are obtained, the origin of which remains somewhat elusive without other supporting[33,36] measurements. However, it will be shown here that by employing an AC technique within these environments a vastly improved set of experimental observations is possible from a single electrochemical measurement. The approach adopted will focus on the simultaneous measurement of the uncompensated resistance[37], the apparent electrode capacitance and the Faradaic current passed at a disk electrode. Figure 1 shows a schematic representation of the electrode, electrochemical ionic atmosphere, sound source and bubbles generated by the sound field deployed. In order to obtain useful information on the cavitation phenomena in question, the technique is shown to be able to resolve changes in these parameters on the microsecond timescale. The technique, described here and explored for the first time with the use of a passive aluminium substrate as a sensor for surface erosion from cavitation[26,27].

Experimental

An aluminium disk electrode was constructed by casting an aluminium wire (250 µm diameter, Advent Research materials) embedded in epoxy resin (Struers, Epofix) inside a stainless steel tube (6 mm OD). The electrode was polished to a mirror-like finish (1 µm and 0.3 µm, Struers, on microcloth, Buehler). The stainless steel outer support was utilised as the reference/counter electrode. The electrode was positioned under a piston-like emitter (PLE) (Microson, 3.2 mm diameter) in a face-on configuration controlled with an XYZ manual stage.

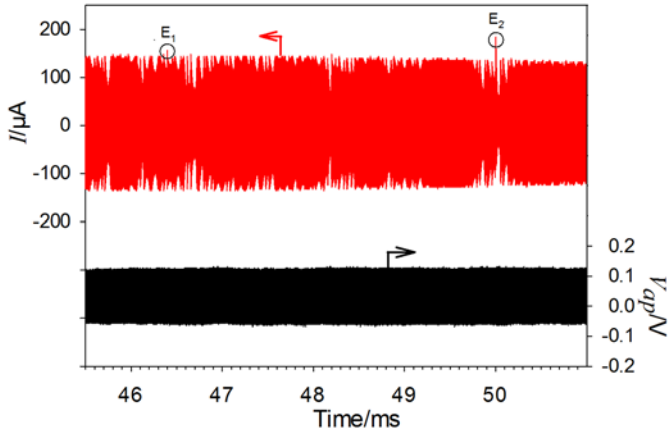

Figure 2. Plots showing the AC excitation voltage (—) and current response (—) recorded for a 250 µm diameter aluminium electrode exposed to ultrasonic cavitation produced by a 3.2 mm diameter tip of an ultrasonic piston-like emitter operating at ~23 kHz. The distance between the tip and the electrode was maintained at 0.7 mm. The aerobic solution contained 0.2 mol dm^{-3} Na_2SO_4 at 19 °C. The labels 'E_1' and 'E_2' correspond to two erosion/ corrosion events detected by the electrode during this time window.

The aluminium disk was aligned to the centre of the tip of the PLE employed (in the horizontal or XY plane) and the Z position was controlled and is reported in the appropriate figure legends. The potential of the working electrode was maintained at 0 V *vs.* the steel reference. An AC perturbation (a 500 kHz sinusoid, 100 mV zero-to-peak amplitude) was applied using a function generator (Handy scope HS3, Tie Pie). A current follower (employing an AD817 opamp, Analogue Devices) was utilised and had a fixed gain of 10^4 V A^{-1}, a high gain bandwidth product (50 MHz) and a small offset (~ +2-4 µA) under these conditions. Both the voltage perturbation and the current passed at the electrode were captured on an oscilloscope (Owon, SDS7102) and transferred to a PC for analysis. A program, which used an FFT analysis routine (National Instruments, Measurement studio), was written (Visual Basic 6) to determine the impedance, the uncompensated resistance (R_u), the capacitance of the electrode (C_e) and the Faradaic current (I_F) every 2 µs from the data recorded. All electrolyte solutions were aerobic and consisted of 0.2 mol dm^{-3} Na_2SO_4 (Fisher Lab reagent used as received) in pure water (Purite, > 15 MΩ cm) at 19 ± 1 °C. In order to measure the effects of cavitation bubbles on the surface of the aluminium electrode, a fixed frequency AC modulation technique was employed. Here the AC perturbation was imposed on the DC bias of the system (0 V *vs.* stainless steel). This was measured to correspond to -0.493 V *vs.* mercury/mercurous sulfate sat. K_2SO_4. The electrochemical response of the electrode was monitored as a function of time by simultaneously recording both the voltage perturbation imposed and the current time history of the electrode. It is important to note that both recorded signals are required in order to elucidate the desired parameters (specifically, the local uncompensated resistance, the electrode capacitance and the Faradaic current). A FFT approach (applied to both the current passed and the applied AC voltage excitation) allows for the magnitude of the frequency components (targeting the 500 kHz signal in particular) and phase angle between these two signals to be gathered. Figure S1 shows a schematic of the approach adopted here. It is important to note that in order for the appropriate information to be extracted from the experimental data, care must be placed on the sample rate in relation to the excitation signal and the time resolution required in the experiment. Here, a sample frequency of 10 MHz was employed and the data was analysed over a 20 data-point window (corresponding to 2 µs in time). This window was stepped through the entire data set to extract the relevant parameters as a function of time. A discussion of calibration experiments and overall accuracy of this technique (compared to a conventional approach) is shown in the SI.

Results

Figure 2 shows a section of the current time and associated voltage excitation captured for an aluminium electrode exposed to inertial (or transient) cavitation. As a result of the time scales employed on the x-axis, this data appears as a block of 'noise'. However, the current time data (here in red, —) shows distinct

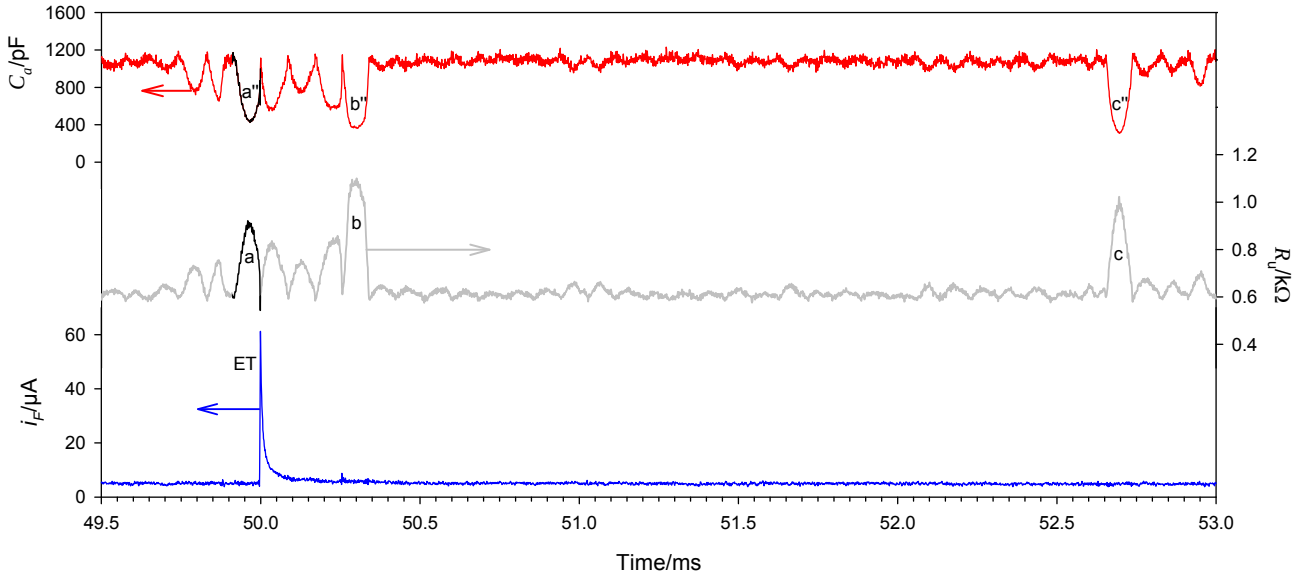

Figure 3. Plots showing the measured capacitance of the electrode (C_a,—), the uncompensated resistance (R_u, —) and Faradaic current (i_F, —) as a function of time calculated from the current time history and voltage perturbations. The highlighted sections (—) and the annotations ('a', 'b', 'c' etc.) refer to bubble events discussed in the text. All experimental conditions are as reported in figure 1. 'ET' represents the single erosion/corrosion transient seen in this time window.

changes in amplitude as a function of time while the excitation voltage (—) remains constant as expected. The changes in the current time signal are a result of the cavitation processes occurring at, or close to, the solid/liquid interface of the aluminium electrode. Two points should be noted; first, although the zero-to-peak amplitude of the current time signal under these conditions is ~150 μA, many reductions in this amplitude can be seen over the ~5.5 ms time window shown; and second, currents in excess of this 150 μA amplitude are also observed but at a far lower rate compared to the reductions in amplitude. Figure 2 shows two such current spike events, labelled '$E_{1,2}$'. In order to elucidate the mechanistic detail contained within this data, it is useful to employ a FFT approach. This enables the magnitudes and phase angles of the signals recorded to be determined. These parameters are then used to extract (see SI figures S1 and S2) the uncompensated resistance of the electrode (R_u), the apparent electrode capacitance (C_a) and the Faradaic signal (I_F) as a function of time. Figure 3 shows the results of such an analysis for an aluminium electrode exposed to cavitation. Figure 3 shows that the apparent capacitance of the electrode was initially ~1100 pF. However, the capacitance falls below this level while the uncompensated resistance increases above a baseline of ~600 Ω in a transient manner. These changes are attributed to the generation, motion and collapse of cavitation bubbles near the electrode surface. The bubbles under these conditions change the environment around the electrode and as a result can be expected to alter the uncompensated resistance etc. as a function of time. Figure 3 shows that for this data set all uncompensated resistance changes are accompanied by capacitance reductions. The data analysis implies that a significant proportion of the apparent capacitance measured using this single frequency AC technique is perturbed during these transient events. However, only the bubble collapse associated with transients labelled **a** and **a''** in figure 3 are responsible for the erosion of the surface which led to the subsequent corrosion transient at 50 ms in figure 3. The current transient (labelled 'ET') occurred directly after bubble collapse (as inferred from the resistance and capacitance transients, **a** and **a''** respectively). Transient **a** corresponds to ~79 μs in duration which is comparable to the periodicity of bubble dynamics[38] in the sound field employed. This is clear evidence that the current transient (I_F) observed here and those reported elsewhere[26,39] are a result of bubble action which in turn induces (visible[26]) surface damage to the electrode. These individual erosion events are accompanied by an anodic current transient[26] as a result of the ensuing passivation of the exposed surface and are not simple charging events. This supports the arguments presented earlier regarding these events[26]. Other resistance and capacitance transients are also seen in figure 3. For example, **b**, **b''** and **c**, **c''** represent just two examples from the set that are presented. However, these transients are not accompanied with a subsequent corrosion transient even though they are of a significant magnitude. Hence these are expected to represent bubble events which, although close to the solid/liquid interface, do not produce conditions sufficient for the erosion of the passive layer on the electrode surface (as depicted by the break in the layer seen under a bubble event on figure 1). Clearly the number of erosion/corrosion events is relatively small compared to the number of capacitance and associated uncompensated resistance changes observed. Further to this, the largest capacitance and resistance events are not necessarily associated with erosion of the interface. This has two important consequences. First, erosion of the passive layer from cavitation close to the interface could be related to position over the interface so that collapse of the bubbles not only needs to occur but needs to be in the correct position with respect to the structure of the passive regions on

the electrode. However, further complimentary evidence would be required to support this proposal. Second, when surface erosion occurs, the shape of the uncompensated resistance (R_u) and apparent capacitance changes (C_a) are as expected from bubble dynamic considerations which also show a marked asymmetric nature. For example, if we compare the uncompensated resistance of the electrode during bubble growth and collapse it is apparent that although bubble growth is rapid (see transient **a** for example), it is still slower than collapse. This is in agreement with the bubble dynamics[1] predicted in these systems and provides further complimentary evidence to support the assumption that these events are linked to the cavitation process itself.

Finally, the technique presented here could be employed in many different systems where transient changes in local impedance are expected (e.g. particle impact, which is important from a technological perspective, and bubble evolution from an interface). This method may have significant benefit and provide mechanistic detail for many complex systems. These are currently under investigation and will be detailed in due course.

Conclusions

A powerful technique able to determine, with a 2 μs temporal resolution, the dynamic changes in the uncompensated resistance and capacitance of an electrode as well as the Faradaic current passed, has been presented. The results indicate that the erosion/corrosion transients reported in the literature are indeed associated with bubble growth and collapse and not capacitance changes themselves.

Acknowledgements

The authors would like to thank the University of Southampton, Chemistry and the Electrochemistry group for support.

Notes and references

1 T. G. Leighton, *The Acoustic Bubble*, Academic Press, London, 1994.
2 C. W. Tobias, *J. Electrochem. Soc.*, 1959, **106**, 833–838.
3 N. P. Brandon and G. H. Kelsall, *J. Appl. Electrochem.*, 1985, **15**, 475–484.
4 G. H. Kelsall, S. Tang, A. L. Smith and S. Yurdakul, *J. Chem. Soc. Faraday Trans.*, 1996, **92**, 3879.
5 S. N. Patek, R. L. Korff and R. L. Caldwell, *Nature*, 2004, **428**, 819–820.
6 S. N. Patek and R. L. Caldwell, *J. Exp. Biol.*, 2005, **208**, 3655–64.
7 A. Kumar, R. B. Bhatt, P. G. Behere and M. Afzal, *Ultrasonics*, 2014, **54**, 1052–6.
8 J. Dickinson, H. Murdoch, M. J. Dennis, G. A. Hall, R. Bott, W. D. Crabb, C. Penet, J. M. Sutton and N. D. H. Raven, *J. Hosp. Infect.*, 2009, **72**, 65–70.
9 S. E. Bilek and F. Turantaş, *Int. J. Food Microbiol.*, 2013, **166**, 155–62.
10 D. G. Offin, P. R. Birkin and T. G. Leighton, *Phys. Chem. Chem. Phys.*, 2014, **16**, 4982–9.
11 K. S. Suslick, D. A. Hammerton and R. E. Cline, *J. Am. Chem. Soc.*, 1986, **108**, 5641–5642.
12 E. B. Flint and K. S. Suslick, *Science (80-.).*, 1991, **253**, 1397–1399.
13 A. Philipp and W. Lauterborn, *J. Fluid Mech.*, 1998, **361**, 75–116.
14 G. E. Reisman, Y.-C. Wang and C. E. Brennen, *J. Fluid Mech.*, 1998, **355**, 255–283.
15 K. S. Suslick, *Science (80-.).*, 1990, **247**, 1439–1445.
16 M. E. Abdelsalam and P. R. Birkin, *Phys. Chem. Chem. Phys.*, 2002, **4**, 5340–5345.
17 A. Kotronarou and M. R. Hoffmann, *J. Phys. Chem.*, 1991, **95**, 3630–3638.
18 R. A. Salkar, P. Jeevanandam, S. T. Aruna, Y. Koltypin and A. Gedanken, *J. Mater. Chem.*, 1999, **9**, 1333–1335.
19 Y. Nagata, Y. Watananabe, S. Fujita, T. Dohmaru and S. Taniguchi, *J. Chem. Soc. Chem. Commun.*, 1992, 1620.
20 P. R. Birkin, D. G. Offin, P. F. Joseph and T. G. Leighton, *J. Phys. Chem. B*, 2005, **109**, 16997–17005.
21 T. G. Leighton, P. R. Birkin, M. Hodnett, B. Zeqiri, J. F. Power, G. J. Price, T. Mason, M. Plattes, N. Dezhkunov, A. J. Coleman, N. Physical, H. Road, C. Down and S. T. Hospital, *Sound Vib.*, 2005, **661**, 37–94.
22 P. R. Birkin, D. G. Offin, C. J. B. Vian and T. G. Leighton, *J. Acoust. Soc. Am.*, 2011, **130**, 3379–3388.
23 M. Hodnett and B. Zeqiri, *Ultrason. Sonochem.*, 1997, **4**, 273–288.
24 R. A. Roy, A. A. Atchley, L. A. Crum, J. B. Fowlkes and J. J. Reidy, *J. Acoust. Soc. Am.*, 1985, **78**, 1799–1805.
25 H. H. Zhang and L. A. Coury, *Anal. Chem.*, 1993, **65**, 1552–1558.
26 P. R. Birkin, R. O'Connor, C. Rapple and S. S. Martinez, *J. Chem. Soc. Faraday Trans.*, 1998, **94**, 3365–3371.
27 P. R. Birkin, D. G. Offin and T. G. Leighton, *Wear*, 2005, **258**, 623–628.
28 F. G. Hammitt, *Cavitation damage and performance Research Facilities*, ASME, New York, 1964.
29 B. Vyas and C. M. Preece, *J. Appl. Phys.*, 1976, **47**, 5133–5138.
30 C. E. Banks and R. G. Compton, 2003, **48**, 159–180.
31 P. R. Birkin and S. Silva-Martinez, *Chem. Commun.*, 1996, **416**, 127–138.
32 P. R. Birkin, D. G. Offin and T. G. Leighton, *Electrochem. commun.*, 2004, **6**, 1174–1179.
33 E. Maisonhaute, P. C. White and R. G. Compton, *J. Phys. Chem. B*, 2001, **105**, 12087–12091.
34 N. P. Brandon and G. H. Kelsall, *J. Appl. Electrochem.*, 1985, **15**, 475–484.
35 P. R. Birkin, Y. E. Watson and T. G. Leighton, *Chem. Commun.*, 2001, 2650–2651.
36 P. R. Birkin, D. G. Offin, C. J. B. Vian, T. G. Leighton and A. O. Maksimov, *J. Acoust. Soc. Am.*, 2011, **130**, 3297–308.
37 J. Fransaer, V. Bouet, J. Celis, C. Gabrielli, E. Huet and G. Maurin, *J. Electrochem. Soc.*, 1995, **142**, 4181–4189.
38 I. Hansson, V. Kedrinskii and K. A. Morch, *J. Appl. Phys. D Appl. Phys.*, 1982, **15**, 1725–1734.
39 P. R. Birkin, D. G. Offin and T. G. Leighton, *Phys. Chem. Chem. Phys.*, 2005, **7**, 530–537.

